Turkish Journal of Electrical Engineering & Computer Sciences

http://journals.tubitak.gov.tr/elektrik/

Research Article

Turk J Elec Eng & Comp Sci
(2017) 25: 3215 – 3226

doi:10.3906/elk-1510-37

A new segmentation method of cerebral MRI images based on the fuzzy c-means algorithm

Mohamed Zaki ABDERREZAK*, Mouatez Billah CHIBANE, Karim MANSOUR
Laboratory for the Study of Electronic Materials for Medical Applications, Department of Electronics Engineering, Frères Mentouri University, Constantine, Algeria

Received: 06.10.2015 • **Accepted/Published Online:** 26.12.2016 • **Final Version:** 30.07.2017

Abstract: The aim of this work is to present a new method for cerebral MRI image segmentation based on modification of the fuzzy c-means (FCM) algorithm. We used local and nonlocal information distance in the initial function of the robust FCM model. The obtained results of the classification of MRI images showed the effectiveness of the suggested model. Calculation of the similarity index confirms that our method is well adapted to MRI images even in the presence of noise.

Key words: Segmentation, magnetic resonance imaging, fuzzy c-means algorithm

1. Introduction

Many acquisition methods exist in medical imaging such as magnetic resonance imaging (MRI), ultrasounds, X-rays (radiography), and photon emission tomography (PET). MRI has undeniable qualities for the contrast and characterization of brain tissues. Segmentation is an important step of medical image processing. It is carried out before the steps of visualization and analysis of anatomical structures.

Several segmentation models have been proposed [1–5]. We can group them into two categories [6]: unsupervised segmentation [7], which aims to automatically separate an image without prior knowledge of classes (i.e. it does not require any training base or any preliminary tasks related to manual labeling), and supervised segmentation, [8] which consists of determining the groups that we wish to achieve before segmentation (i.e. segmentation by Markov's fields [2] and neural networks [3]). In our work, we will limit the study to fuzzy c-means (FCM) segmentation, introduced by Pham et al. [9], which is based on the fuzzy unsupervised classification algorithm. Each point in the data set belongs to a cluster with a certain degree. All the clusters are characterized by their gravity center. Weijie and Giger [10] and Singh et al. [11] adapted this segmentation for MRI image segmentation. Brandt et al. [12] used the segmentation to measure cranial spinal liquid volume, white matter, and gray matter in pediatric brain MRIs. Clark et al. [13] used it as a stage of initialization in an expert system in order to segment tumor volumes or edema on cerebral MRI images. Menon and Ramakrishnan used it to segment tumors [14].

Segmentation FCM is used in cerebral MRI image analysis [15]. Its flexibility allows the pixel to belong to several classes; it provides good repair performance in the presence of the partial volume effect [16]. However, the standard FCM algorithm does not compensate for intensity inhomogeneities [17]. To overcome this problem,

*Correspondence: zaki.abderrezak@gmail.com

several approaches were proposed [6,18–20]. Pham [18] proposed a robust method that takes into account only the membership functions of the voxel neighbor in order to force the segmentation using a regulating term in the standard function. Several other models were proposed for the same purpose. Sahbi and Nozha [21] introduced a regulating term based on entropy. Sathya et al. [22] used a quadratic regulating term. Wang et al. [23], Cai et al. [24], Ahmed et al. [25], and Bazin and Pham [26] incorporated special information in the regulating term. The limits of the proposed improvements have led us to introduce in our method an approach that can minimize noise sensitivity while taking into account the spatial information of pixels.

The aim of our work is to study the FCM and robust FCM (RFCM) models introduced by Pham [18]. We will then present our approach and the results obtained from brain MRIs by comparing them to those obtained by other approaches.

2. Methods

The classic FCM segmentation algorithm was applied successfully to several classification varieties. The FCM standard algorithm can be described by the following theory.

Let us consider that $X = \{x_j / x_j \in R,\ j \in \{1, \dots n\}\}$ is a vector space where $n \in N$ represents the number of pixels in the image and $V = \{v_i / v_i \in R, i \in \{1, ..., c\}\}$ is a prototype vector space that characterizes the classes, where $c,\ c \in N$ represents the number of classes $(1 < c < n)$. In the FCM segmentation case, x_j is not assigned to a single class, but rather to several classes via different degrees of membership u_{ji}. The aim of the classification algorithm is not only to calculate the centers of a class v_i, but also to determine all degrees of membership to the classes of the vectors.

$U = \{u_{ji} / u_{ji} \in R^{n \times c}, j \in \{1, ..n\}, i \in \{1, ..., c\}\}$ represents the fuzzy separation matrix that should satisfy the following conditions:

$$0 \leq u_{ji} \leq 1 \quad \forall i \in [1, c], \forall j \in [1, n] \tag{1}$$

$$\sum_{i=1}^{c} u_{ji} = 1 \quad \forall j \in [1, n]\ Closure\, relation \tag{2}$$

$$0 < \sum_{j=1}^{n} u_{ji} < n \quad \forall i \in [1, c]\ No\, empty\, class \tag{3}$$

The function of energy connecting the partition u_{ji} to the prototypes v_i is defined by:

$$J(u, v) = \sum_{j=1}^{n} \sum_{i=1}^{c} u_{ij}^{q} d^2(x_j, v_i) \tag{4}$$

where $q > 1$ is the fuzzy degree of the segmentation.

We can then search the optimal partitioning $(c_1 c_2 c_n)$ and the optimal prototype to minimize Eq. (4) by using the following theorem [4]:

Fuzzy c-means theorem. To carry out a partitioning $(c_1 c_2 c_n)$, we must minimize Eq. (4) of the energy by using the following Lagrange function:

$$J_L = J(u, v) + \sum_{j=1}^{n} \lambda_j \left(1 - \sum_{i=1}^{c} u_{ji}\right) \tag{5}$$

with the following conditions:

$$\frac{\partial}{\partial u_{ji}} J_L = 0 \tag{6}$$

$$\frac{\partial}{\partial v_i} J_L = 0 \tag{7}$$

λ_j represents Lagrange's multiplier, which is calculated after the calculation of the derivates of Eqs. (6) and (7). The membership degrees u_{ji} and the centroid v_i must satisfy the following conditions:

$$u_{ji} = \left[\sum_{k=1}^{c} \left(\frac{d\left(x_j, v_i\right)}{d\left(x_j, v_k\right)} \right)^{2/(q-1)} \right]^{-1} \qquad 1 \leq i \leq c, \quad x_i \in X \tag{8}$$

$$v_i = \frac{\sum_{j=1}^{n} u_{ij}^{q} x_j}{\sum_{j=1}^{n} u_{ij}^{q}} \qquad 1 \leq i \leq c \tag{9}$$

The term $d^2\left(x_j, v_i\right)$ calculates the similarity between x_j and v_i :

$$d^2\left(x_j, v_i\right) = \left\| x_j - v_i \right\|^2 \tag{10}$$

where $\|.\|$ represents the Euclidean distance.

This theorem makes possible the determination of the prototypes and the membership function in an iterative way by using Eq. (8) and Eq. (9) until a criterion of convergence is reached.

The FCM algorithm requires prior knowledge of the class number and generates these classes through an iterative process to minimize the function of energy. This produces a fuzzy partition in the image by giving each pixel a degree of membership in a given class (from 1 to 0). The class that is associated with a pixel is the one whose degree is the highest. The FCM algorithm stages are as follows:

Input: Image, $x = \{x_1, x_2, \ldots, x_n\}$ the number of the class c, to fix q a value such as $q > 1$, to fix the threshold of convergence.

Step 1: Initialize the matrix of partition $U = [u_{ji}]$

Step 2: Initialize the counter $t = 0$.

Step 3: Calculate the value of centroid v_i^t using Eq. (9).

Step 4: Calculate u_{ji}^{t+1} for $j = 1 \, to \, n$

I_j the set of values i that satisfied $I_j = \left\{ i / 1 \leq i \leq c, d_{ji} = \|x_j - v_i\| = 0 \right\}$

If $I_j = \emptyset \, then$

calculate u_{ji}^{t+1} with Eq. (8)

Else $u_{ji}^{t+1} = 0$

For all $i \notin I$ and $\sum_{i \in I_j} u_{ji}^{t+1} = 1$, continue with another j.

Step 5: if $\left\| U^t - U^{t+1} \right\| < \varepsilon$, then stop. If not, set $t = t + 1$ and go to step 3.

One of the disadvantages of FCM segmentation is its sensitivity to the intensity of heterogeneities because the centroids are invariants in the image space, from where the interest to modify the standard function of energy appears.

To adapt the FCM model to the presence of artifacts, several approaches were proposed, one of which is the addition of a regulating term to the initial FCM function. Pham [18] proposed an extension to the FCM algorithm. The function is then written as follows:

$$J = \left(\sum_{j=1}^{n}\left(\sum_{i=1}^{c} u_{ji}\left\|x_j - v_i\right\|_2^2\right)\right) + \frac{\beta}{2}\left(\sum_{j=1}^{n}\sum_{i=1}^{c} u_{ji}^{q}\left(\sum_{k\in N_j^R}\sum_{l\in L_i} u_{kl}^{q}\right)\right) \tag{11}$$

The first term represents the initial function of FCM, which is also called a data fidelity term; the second term is a regulating term of the energy function.

$\left\|x_j - v_i\right\|_2^2$ is the Euclidean distance, N_j^R is a neighborhood of voxel j, β is a constant that controls the respective weights between the fastener term to the data and the regulation, $L_i = [1,c]/\{i\} = \{1,...,i-1,i+1,\dots c\}$, and v_i make up the centroid.

Our approach is based on the work of Caldairou et al. [27]. We used a nonlocal weight $w_{nl}(k,j)$ in the two terms of Eq. (11) to select the most relevant voxels within the zone of search. It is then possible to carry out a regulation according to the similarity degree. We also used the local and nonlocal distance presented by Wang et al. [23]. Wang et al. modified the initial FCM function by weighting local information and nonlocal information and by redefining the distance between the intensity of a voxel and the centroid of a class. In our model, we combined the two methods to retain the advantages of both. A nonlocal weight was first introduced in the regulating term of the function to take into account the voxel vicinity in the membership function calculation of voxel j of the class c in order to minimize the influence of noise intensity. We then used a local and a nonlocal weight in the calculation of the distance between voxel j and the centroid.

The new function is then written as:

$$J = J_{FCM} + J_{Reg}$$

$$J = \sum_{j=1}^{n}\left(\sum_{i=1}^{c} u_{ji}\left(\sum_{k\in N_j} w_{kj}D^2(x_j,v_i)\right)\right) + \frac{\beta}{2}\left(\sum_{j=1}^{n}\left(\sum_{i=1}^{c} u_{ji}^{q}\right)\sum_{k\in N_j^R} w_{kj}\left(\sum_{l\in L_i}\sum_{k\in N_j} u_{kl}^{q}\right)\right) \tag{12}$$

To minimize Eq. (12), the Lagrange function of Theorem 1 is used.

$$\frac{\partial J}{\partial u_{ji}} = q u_{ji}^{q-1}\left(\sum_{k\in N_j}\left(w_{kj}D^2(x_j,v_i)\right) + \beta\left(\sum_{k\in N_j} w_{kj}\right)\left(\sum_{l\in L_i}\sum_{k\in N_j} u_{kl}^{q}\right)\right) - \lambda_j \tag{13}$$

Using Eq. (6), we obtain:

$$u_{ji} = \frac{\left(\sum\limits_{k\in N_j} w_{kj}D^2(x_j,v_i) + \beta\sum\limits_{k\in N_j} w_{kj}\sum\limits_{k\in N_j}\sum\limits_{l\in L_i} u_{kl}^{q}\right)^{-1/(q-1)}}{\sum\limits_{i=1}^{c}\left(\sum\limits_{k\in N_j} w_{kj}D^2(x_j,v_i) + \beta\sum\limits_{k\in N_j} w_{kj}\sum\limits_{k\in N_j}\sum\limits_{l\in L_i} u_{kl}^{q}\right)^{-1/(q-1)}} \tag{14}$$

$D^2(x_j,v_i)$ represents the distance between the intensity x_j of voxel j and the centroid v_i of class i. It is a combination of a local distance and nonlocal distance [23] calculated using:

$$D^2(x_j,v_i) = (1-\varphi_j)\, d_l^2(x_j,v_i) + \varphi_j d_{nl}^2(x_j,v_i) \tag{15}$$

φ_j locally controls the proportion between the distances d_l and d_{nl} for the calculation of the final distance D. d_l measures the distance influenced by the local information calculated by the following expression:

$$d_l^2(x_j,v_i) = \frac{\sum\limits_{x_k \in N_j} w_l(x_k,x_j)\, d^2(x_k,v_i)}{\sum\limits_{x_k \in N_i} w_l(x_k,x_j)} \tag{16}$$

where N_j is a neighborhood centered around voxel j, and $d^2(x_k v_i)$ represents the Euclidean distance. w_l is the local weight of each pixel in N_i defined by:

$$w_l(x_k,x_j) = e^{-\frac{|x_k - x_j|^2}{\delta^2}} \tag{17}$$

δ^2 is the variance of N_i, and d_{nl} is the distance influenced by the nonlocal information of all the pixels in the given image I, which is calculated by:

$$d_{nl}^2(x_j,v_i) = \sum_{x_k \in I} w_{nl}(x_k,x_j)\, d^2(x_k,v_i) \tag{18}$$

$$w_{nl}(x_k,x_j) = \frac{1}{Z(x_j)} U(x_k,x_j) \tag{19}$$

$U(x_k,x_j)$ is the exponential form of the similarity:

$$U(x_k,x_j) = e^{-\frac{\|V(N_k)-V(N_j)\|_{2,a}^2}{h^2}} \tag{20}$$

The similarity between the two pixels x_k *and* x_j is calculated by the Euclidean distance $\|V(N_k) - V(N_j)\|_{2,a}^2$, where $V(N_k)$ and $V(N_j)$ represent the pixels' intensities. The parameter h governs the smoothing degree of the nonlocal filtering, and $Z(x_j)$ is a constant of standardization:

$$Z(x_j) = \sum_{x_k \in I} e^{-\frac{\|V(N_k)-V(N_j)\|_{2,a}^2}{h^2}} \tag{21}$$

$$\varphi_j = \frac{1}{q} \sum_{i=1}^{q} U_i(x_k,x_j) \tag{22}$$

The proposed algorithm is:

Input: Image, $X = \{x_1, x_2, \ldots, x_n\}$ the number of the classes c, q and set $\varepsilon > 0$

Step 1: Compute w_{kj} for all $(kj) \in \Omega^2$.

Step 2: Initialization of the centroids $V = [v_1, v_2, \ldots\ldots v_c]$

Step 3: Calculate the new distance with Eq. (15).

Step 4: Update the value of u_{ji} using Eq. (14).

Step 5: Update v_i using Eq. (9).

Step 6: Repeat Steps 3–5 until the following termination criterion is met:

$$\|v_{new} - v_{old}\| < \varepsilon.$$

The algorithm was implemented in MATLAB R2013a using Windows 7 with an Intel Core i3 2.30 GHz processor and 4.00 GB of RAM.

3. Results

Our model was applied to synthesized images consisting of real MRIs obtained from the Internet Brain Segmentation Repository (IBSR) provided by the Center for Morphometric Analysis at Massachusetts General Hospital. The algorithm was applied on clinical MRI images. The obtained results were compared to those generated by other segmentation methods such as FCM and FCMS proposed by Ahmed et al. [25] and RFCM suggested by Pham et al. [18].

The program was applied to a synthetic 2D image (435×335) in the presence of Gaussian noise with a deviation equal to 9. We fixed $q = 2\,, C = 3,$ and $h = 2\alpha\sigma^2 \left|P_j^I\right|$. The Coupé approach [28] produces better results for brain MRI segmentation with a patch size of $\left|P_j^I\right|$. σ represents the standard deviation of noise and $\alpha = 2$ and $\varepsilon = 1e - 5$ during all handling. Figures 1a, 1b, 1c, 1d, 1e, and 1f represent, respectively, the image to be segmented, the disturbed image, FCM segmentation, FCMS segmentation, segmentation with the standard model RFCM, and segmentation with our model. After several trials, we fixed $\beta = 500$ with a neighborhood (3×3). For the FCMS model, it was $\alpha = 2$. The obtained results show that our method is more effective than the other methods in the presence of Gaussian noise. To evaluate the performance of our segmentation, we calculated three indices: the similarity index ρ, the number of false-positives r_{fp}, and the number of false-negatives r_{fn} [29]. ρ is represented by the following equation:

$$\rho = \frac{2\,|A_i \cap B_i|}{|A_i| + |B_i|} \tag{23}$$

The similarity index is a positive value that represents the correspondence of the pixels in the two images A (manually segmented image) and B (a segmented image using our approach). A_i and B_i represent the pixels of class i during manual segmentation and in the segmentation carried out by our method, respectively. $|A_i|$ is the number of pixels in image A, and $|B_i|$ is the number of pixels in image B. An excellent similarity is obtained when $\rho > 70\%$ [29]. To calculate the number of false-positives and false-negatives, we used the following equations:

$$r_{fp} = \frac{|B_i| - |A_i \cap B_i|}{|A_i|} \tag{24}$$

$$r_{fn} = \frac{|A_i| - |A_i \cap B_i|}{|A_i|} \tag{25}$$

The false-positives rate measures the capacity of the algorithm to oversegment the images. In other words, the pixel is included in the segmentation but not in the reference segmentation. The false-negatives rate measures

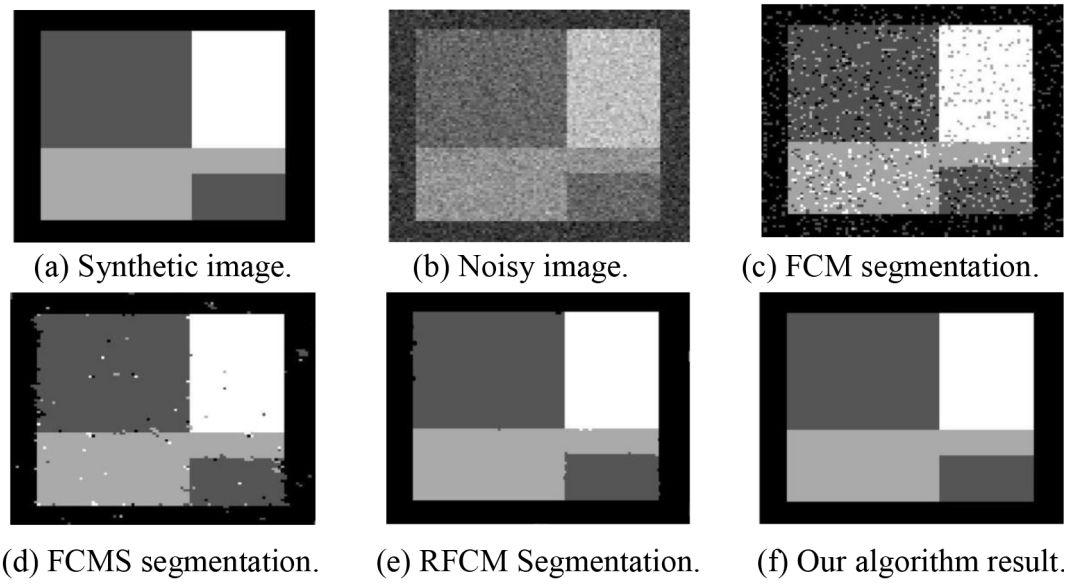

Figure 1. Segmentation of a synthetic image: a) synthetic image, b) noisy image, c) FCM segmentation, d) FCMS segmentation, e) RFCM segmentation, f) the result of our algorithm.

its capacity to undersegment the images, i.e. the pixel is excluded from the segmentation but remains in the reference segmentation.

The Table gives the values of the three indices $(\rho, r_{fp} r_{fn})$ for different segmentation methods. Comparison of these values shows the superiority of our method for segmentation of synthetic images.

Table. Values of the similarity index and the rates of false-positives and false-negatives.

	Synthetic image (Figure 1)				MRI image from IBSR (Figure 2)					
					WM (white matter)			GM (gray matter)		
Methods	Δt (s)	ρ%	r_{fp}%	r_{fn}%	ρ%	r_{fp}%	r_{fn}%	ρ%	r_{fp}%	r_{fn}%
FCM	16.42	77.43	23.40	17.35	75.18	20.15	9.87	74.69	8.20	20.98
FCMS	22	92.33	3.40	1.90	88.6	17.65	7.59	85.12	6.07	19.35
RFCM	36.59	99.86	0.51	3.09	90.03	14.98	6.44	86.57	5.63	17.25
Our model	47.39	99.91	0.23	1.61	93.12	8.36	4.68	90.37	3.67	12.03

We used the Brain Extraction Tool [30] to separate brain from nonbrain tissue in all MRI images. Our algorithm was applied to 17 real brain MRI data sets obtained from the IBSR. Figure 2a illustrates the real T1-weighted MRI brain volume of case 8 in the IBSR database. These images have a size of $256 \times 256 \times 128$ voxels and a resolution of $10 \times 10 \times 15$ mm. For all methods, we applied segmentation in three classes representing white matter (WM), gray matter (GM), and the cerebrospinal fluid (CSF) by the FCM method (Figure 2b), by FCMS (Figure 2c), and by RFCM (Figure 2d). The obtained results can be compared to those provided by manual segmentation obtained from the IBSR in order to validate them (Figure 2e). Figure 2f shows the obtained results with the suggested model. The similarity indices, false-negatives and false-positives of WM and GM from the segmentation results in Figure 2 are shown in the Table. The average similarities of WM and GM obtained by the algorithm in our model are larger than 90%. Therefore, our algorithm seems to perform better than the other methods, namely FCM and RFCM. Moreover, it eliminates the noise effect. For this experiment,

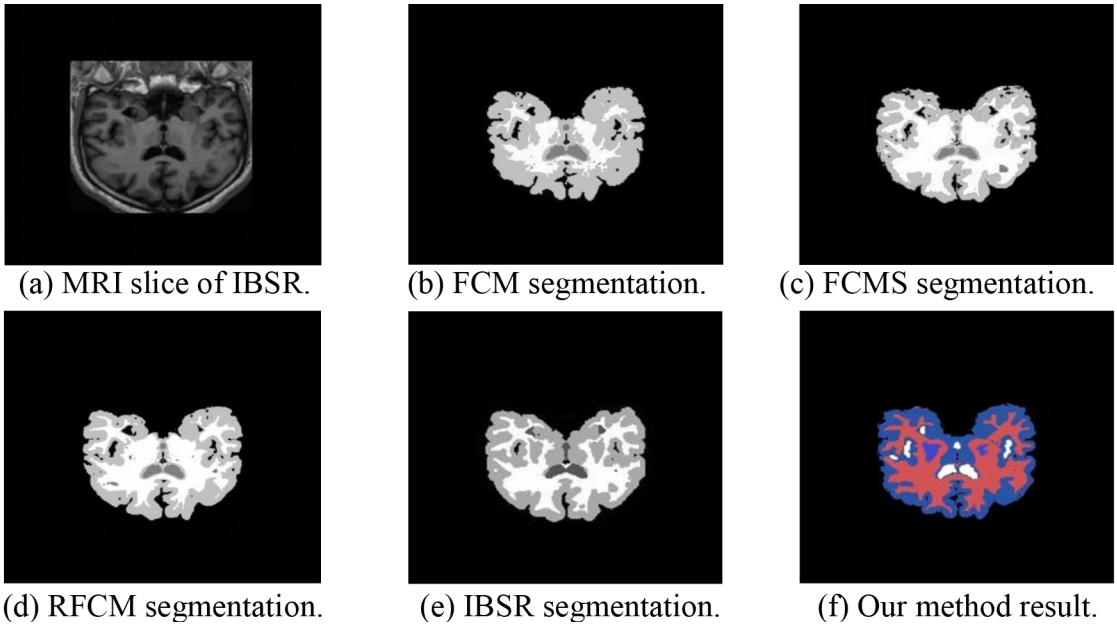

Figure 2. Segmentation of a real MRI image from IBSR: a) MRI slice of IBSR, b) FCM segmentation, c) FCMS segmentation, d) RFCM segmentation, e) IBSR segmentation, f) result of our method.

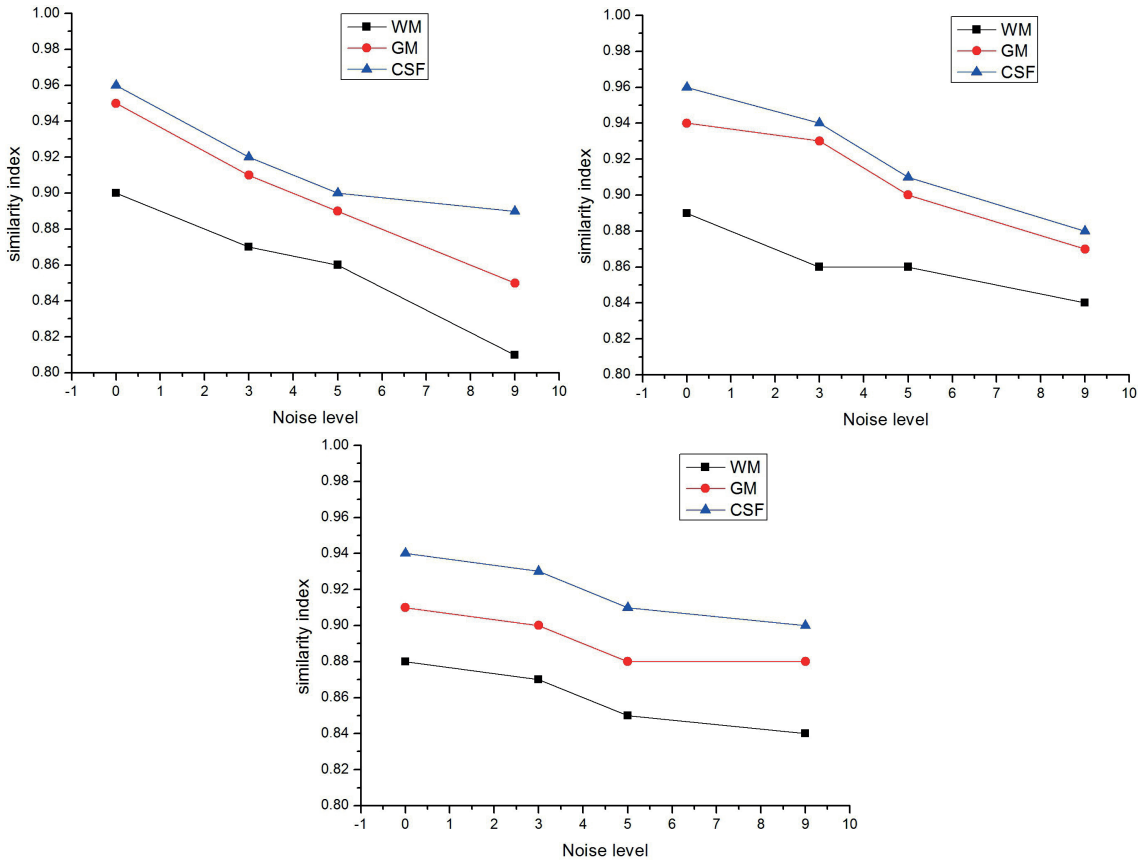

Figure 3. Influence of neighborhood size and noise intensity on the segmentation: a) segmentation with 3 × 3 window, b) segmentation with 5 × 5 window, c) segmentation with 7 × 7 window.

the number of neighborhoods is 7×7 pixels and the execution time is 18 min. This time can be justified by the computation of the nonlocal weights in the data and the regularization terms using a different size of the neighborhood window for each iteration.

In the following section, we study the influence of the neighborhood and noise on the suggested model using IBSR images. Various values of the window size of the neighborhood have been studied with the aim of classification (WM, GM, and CSF) (Figure 3). In Figures 3a and 3b, we used neighborhood windows of 3×3

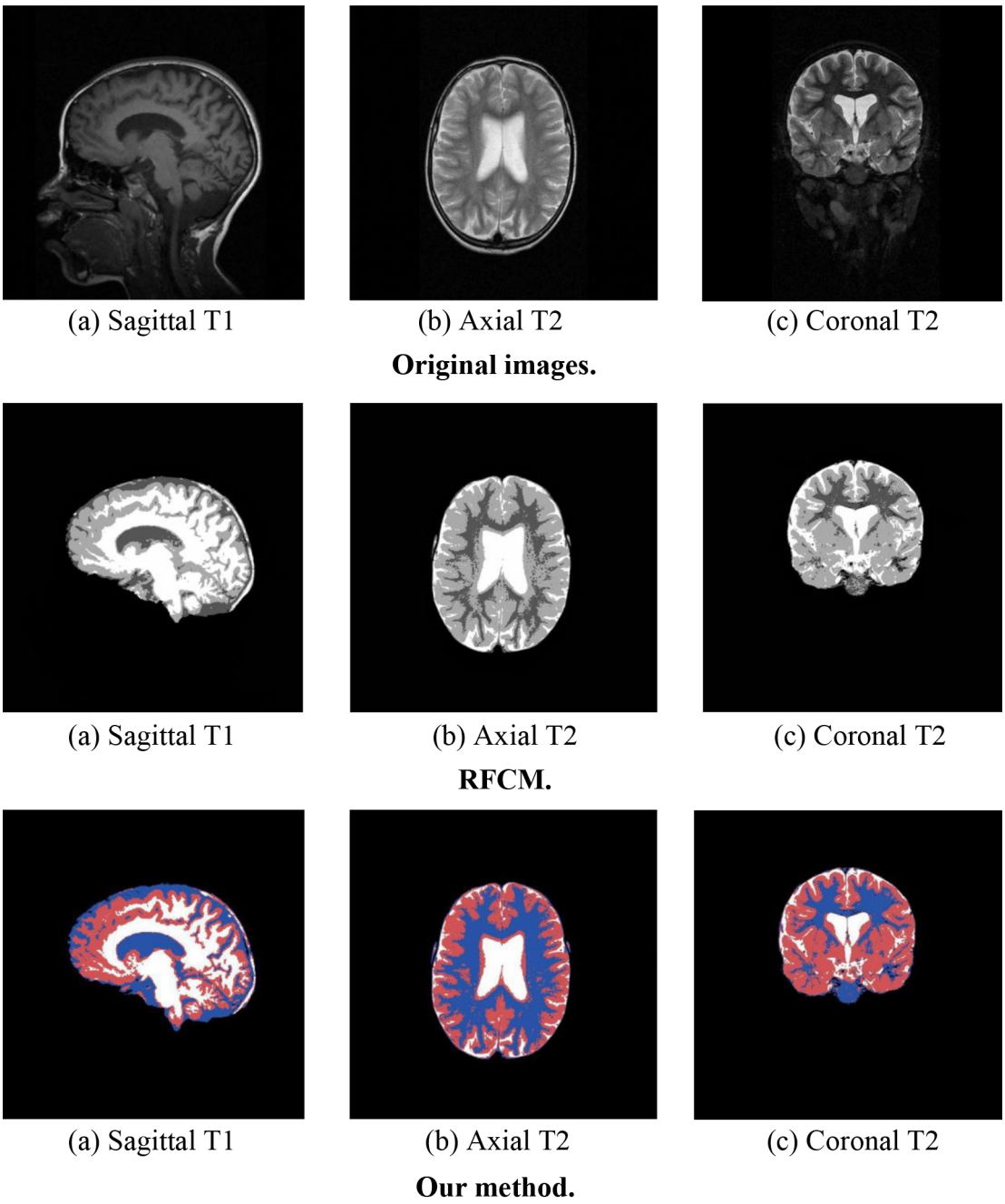

Figure 4. Segmentation results for real brain MRI images.

and 5×5, respectively. In Figure 3c, the similarity index of our model is presented for different values of noise using a neighborhood window size of 7×7.

The curves of Figure 3 show that the similarity index decreases when the noise level increases. This reduction is slowed down by the best choice of the window size of the neighborhood. A comparison of the three figures shows that:

- For CSF, calculation of the similarity index with maximum noise and a neighborhood of 3×3 produces better results than those obtained without noise for a neighborhood of 5×5 or 7×7.
- For GM, we noted that the window size of 5×5 is the best. This finding is based on two criteria: the maximum value of the similarity index (96% for a neighborhood of 5×5) and noise influence on this same value ($> 1\%$ for a neighborhood of 5×5).
- For WM, the three figures show that 7×7 is the optimal window size of the neighborhood in order to obtain the best similarity index (the same criteria used for GM).

We tested our algorithm on 14 cases of T1 and T2 MRI brain images for different modalities obtained from clinical tests. Figure 4a represents a T1 sagittal, Figure 4b represents a T2 axial, and Figure 4c represents a coronal T2. The size of the images tested is $512 \times 512 \times 128$ at $0.5 \times 0.5 \times 3$ resolution.

Figure 4 shows the effectiveness of our method in the segmentation of T1 and T2 MRI images. The best segmentation takes place in the narrow and winding areas, such as the areas between the CSF and GM and also in the region between the GM and WM. These results also show a clearer and more specific delineation of the different regions.

4. Conclusion

In this paper, we showed that our method produces better results for the segmentation of a disturbed cerebral MRI image than those obtained through more classic techniques. This comparison is based on the calculation of the similarity index and the false-positives and false-negatives rates. We also showed that the best choice of the segmentation parameters depends on the brain region that we want to extract.

References

[1] Eun SJ, Whangbo TK. Brain segmentation using susceptibility weighted imaging method. In: IEEE 2014 IT Convergence and Security Conference; 28–30 October 2014; Beijing, China. New York, NY, USA: IEEE. pp. 1-3.

[2] Liang Z, Wang S. An EM approach to MAP solution of segmenting tissue mixtures: a numerical analysis. IEEE T Med Imaging 2009; 28: 297-310.

[3] Meghana N, Rekha KR. Artificial neural network based classification of brain tumor from MRI using FCM and boundring box method. International Journal of Engineering Research and Technology 2015; 4: 982-985.

[4] Bezdek JC, Ehrlich R, Full W. FCM: The fuzzy c-means clustering algorithm. Comput Geosci 1984; 10: 191-203.

[5] Siddiqui FU, Isa NA, Yahya A. Outlier rejection fuzzy c-means (ORFCM) algorithm for image segmentation. Turk J Electr Eng Co 2013; 21: 1801-1819.

[6] Guerra L, McGarry LM, Robles V, Bielza C, Larranaga P, Yuste R. Comparison between supervised and unsupervised classifications of neuronal cell types: a case study. Dev Neurobio 2011; 71: 71-82.

[7] Chabrier S, Emile B, Laurent H, Rosenberger C, Marche P. Unsupervised evaluation of image segmentation application to multi-spectral images. In: IEEE 2004 Pattern Recognition Conference; 23–26 August 2004; Cambridge, UK. New York, NY, USA: IEEE. pp. 576-579.

[8] Vasconcelos M, Vasconcelos N, Carneiro G. Weakly supervised top-down image segmentation. In: IEEE 2006 Computer Vision and Pattern Recognition Conference; 17–22 June 2006; New York, NY, USA. New York, NY, USA: IEEE. pp. 1001-1006.

[9] Pham D, Prince JL, Dagher AP, Xu C. An automated technique for statistical characterization of brain tissues in magnetic resonance imaging. Int J Pattern Recogn 1997; 11: 1189-1211.

[10] Weijie C, Giger ML. A fuzzy c-means (FCM) based algorithm for intensity inhomogeneity correction and segmentation of MR images. In: IEEE 2004 Biomedical Imaging; 15–18 April 2004; Arlington, VA, USA. New York, NY, USA: IEEE. pp. 1307-1310.

[11] Singh P, Bhadauria HS, Singh A. Automatic brain MRI image segmentation using FCM and LSM. In: IEEE 2014 Reliability Infocom Technologies and Optimization Conference; 8–10 October 2014; Noida, India. New York, NY, USA: IEEE. pp. 1-6.

[12] Brandt ME, Fletcher JM, Kramer LA. Brain tissue volumes estimated from magnetic resonance scans in pediatric hydrocephalus. In: IEEE 2002 Biomedical Engineering Society Conference; 23–26 October 2002; Houston, TX, USA. New York, NY, USA: IEEE. pp. 1122-1123.

[13] Clark MC, Hall LO, Goldgof DB, Clarke LP, Velthuizen RP, Silbiger MS. MRI segmentation using fuzzy clustering techniques. IEEE Eng Med Biol 1994; 13: 730-742.

[14] Menon N, Ramakrishnan R. Brain tumor segmentation in MRI images using unsupervised artificial bee colony algorithm and FCM clustering. In: IEEE 2015 Communications and Signal Processing Conference; 2–4 April 2015; Melmaruvathur, India. New York, NY, USA: IEEE. pp. 6-9.

[15] Venu N, Anuradha B. A Novel multiple-kernel based fuzzy c-means algorithm with spatial information for medical image segmentation. Int J Image Processing 2013; 7: 286-301.

[16] Tohka J, Zijdenbos A, Evans A. Fast and robust parameter estimation for statistical partial volume models in brain MRI. Neuroimage 2004; 23: 84-97.

[17] He R, Datta S, Rao Sajja B, Mehta M, Narayana P. Adaptive FCM with contextual constrains for segmentation of multi-spectral MRI. In: IEEE 2004 Engineering in Medicine and Biology Society Conference; 1–5 September 2004; Los Alamitos, CA, USA. New York, NY, USA: IEEE. pp. 1660-1663.

[18] Pham DL. Spatial models for fuzzy clustering. Comput Vis Image Und 2001; 84: 285-297.

[19] Wang ZM, Soh YC, Song Q, Sim K. Adaptive spatial information-theoretic clustering for image segmentation. Pattern Recogn 2009; 42: 2029-2044.

[20] Xue JH, Philips W, Pizurica A, Lemahieu I. A novel method for adaptive enhancement and unsupervised segmentation of MRI brain image. In: IEEE 2001 Acoustics Speech and Signal Processing Conference; 7–11 May 2001; Salt Lake City, UT, USA. New York, NY, USA: IEEE. pp. 2013-2016.

[21] Sahbi H, Nozha B. Validity of fuzzy clustering using entropy regularization. In: IEEE 2005 Fuzzy Systems Conference; 22–25 May 2005; Reno, NV, USA. New York, NY, USA: IEEE. pp. 177-182.

[22] Sathya A, Senthil S, Samuel A. Segmentation of breast MRI using effective fuzzy c-means method based on support vector machine. In: IEEE 2012 Information and Communication Technologies Conference; 30 October–2 November 2012; Trivandrum, India. New York, NY, USA: IEEE. pp. 67-72.

[23] Wang J, Kong J, Lu Y, Qi M, Zhang B. A modified FCM algorithm for MRI brain image segmentation using both local and non-local spatial constraints. Comput Med Imag Grap 2008; 32: 685-698.

[24] Cai W, Chen S, Zhang D. Fast and robust fuzzy c-means clustering algorithms incorporating local information for image segmentation. Pattern Recogn 2007; 40: 825-838.

[25] Ahmed MN, Yamany SM, Mohamed N, Farag AA, Moriarty T. A modified fuzzy c-means algorithm for bias field estimation and segmentation of MRI data. IEEE T Med Imaging 2002; 21: 993-999.

[26] Bazin PL, Pham DL. Topology-preserving tissue classification of magnetic resonance brain images. IEEE T Med Imaging 2007; 26: 487-496.

[27] Caldairou B, Rousseau F, Passat N, Habas PA, Studholme C, Heinrich C. A non-local fuzzy segmentation method: application to brain MRI. Lect Notes Comp Sci 2009; 5702: 606-613.

[28] Coupe P, Yger P, Prima S, Hellier P, Kervrann C, Barillot C. An optimized blockwise nonlocal means denoising filter for 3-D magnetic resonance images. IEEE T Med Imaging 2008; 27: 425-441.

[29] Zijdenbos AP, Dawant BM. Brain segmentation and white matter lesion detection in MR images. Crit Rev Biomed Eng 1994; 22: 401-465.

[30] Smith SM. Fast robust automated brain extraction. Hum Brain Mapp 2002; 17: 143-155.